The Journal of Physical Chemistry A

 VOLUME 101, NUMBER 18, MAY 1, 1997

LETTERS

Photodetached Spin-Polarized Quasi-Free Electrons in Rubidium−Tetrahydrofuran. Dependence of Electron Spin Relaxation upon Wavelength of Excitation

Vladimir Rozenshtein, Yehuda Heimlich, and Haim Levanon*

Department of Physical Chemistry and the Farkas Center for Light-Induced Processes, The Hebrew University of Jerusalem, Jerusalem 91904, Israel

Received: August 22, 1996; In Final Form: March 17, 1997[⊗]

Longitudinal spin relaxation time of electrons photodetached from rubidium anion (Rb^-) in tetrahydrofuran (THF) solution was found to depend on the excitation wavelength (λ = 532, 640, and 720 nm). Spin relaxation rate vs photon energy exhibits a parabolic dependence, which corresponds to the conduction band profile of THF. This unique behavior is attributed to the spin-polarized photoelectrons interacting with rubidium atoms ($Rb^•$) generated in the same photoprocess. Analysis of the results suggests that the photoelectrons exhibit high mobility, an essential feature for spin injection through interfaces.

Introduction

Spin electronics is based on electron spin transfer through interfaces,[1] where spin is carried over from one site to another, similar to charge transfer through interfaces in semiconductors. Experiments indicate that injection of spin-polarized photoelectrons (e_p^-) generated in rubidium−tetrahydrofuran (Rb/THF) solutions through the liquid−metal interface is feasible by applying an electric field across platinum electrodes.[2] The inverse relation between the yield of the spin-polarized photoelectrons and the voltage is indicative of high-mobility electrons. It also confirms previous results showing the different physical properties of e_p^- as compared to low-mobility solvated electrons, e_s^-.[3−5]

In this communication we present a new approach of elucidating the physical nature of e_p^- by investigating its electron spin relaxation and relating the results with the phenomenon of spin injection through interfaces.

Experimental Section

EPR experiments were carried out on a Bruker ESP-380 pulsed EPR spectrometer interfaced to a dye laser (Continuum, TDL-60) pumped by Nd:YAG laser (Continuum, 661-2D) producing a 20 Hz pulse rate of 12 ns duration and an energy of 0.01 J/pulse. For a detailed description of sample preparation and EPR detection, see earlier studies.[3,5,6] Three Rb/THF samples with the same metal concentration (10^{-4} M) were investigated. Each sample was examined at three different wavelengths of photoexcitation, λ = 532, 640, and 720 nm, and for each wavelength, 3−4 runs were carried out.

Results and Discussion

Typical time-dependent spectra of e_p^- formed by photoexcitation of Rb/THF solution (λ = 640 nm) are shown in Figure 1a. All spectra are in emission with a line width of ∼0.2 MHz, in agreement with previous results.[3,5] The same behavior was observed for the other wavelengths used. The temporal behavior of the spectra (Figure 1a) shows that the EPR signal disappears within a few tens of microseconds, and the ratio between the highest and the equilibrium values of spin polarization is ∼30.[5] Figure 1b shows the dependence of the normalized EPR signal intensities, I/I_0, vs the delay times between the laser pulse and microwave detection, τ_d. The values of I_0 were taken at τ_d = 1 μs in order to escape instrumental and polarization buildup

[⊗] Abstract published in *Advance ACS Abstracts,* April 15, 1997.

S1089-5639(96)02610-2 CCC: $14.00

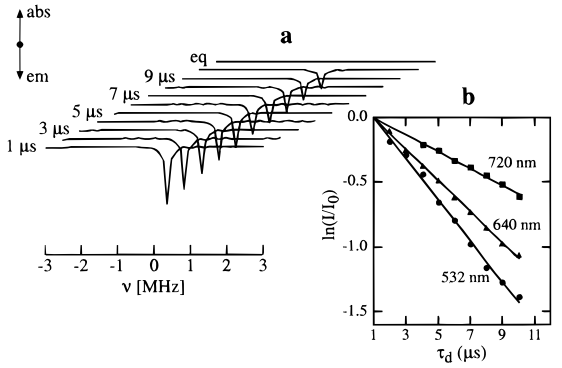

Figure 1. (a) FT-EPR spectra of e_p^- (in emission) taken at different delay times between the laser pulse and microwave detection, τ_d. All spectra were taken at $T = 180$ K and $\lambda = 640$ nm. Similar spectra were obtained at other wavelengths. (b) Normalized signal intensities vs τ_d, taken at three wavelengths of photoexcitation. Solid lines are curves employing eq 1.

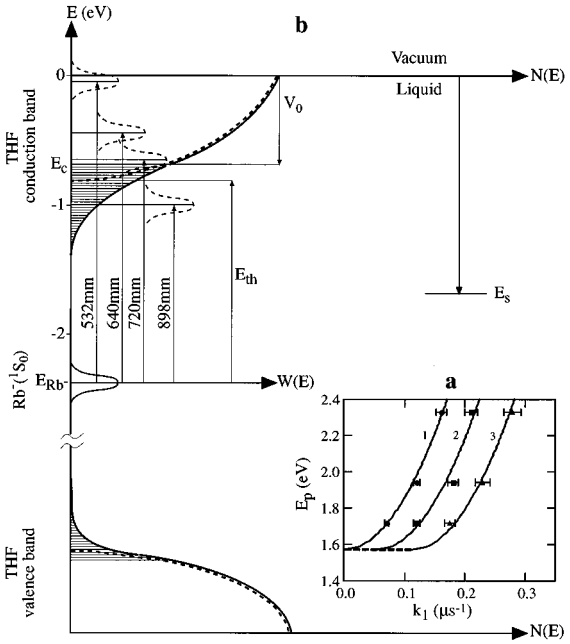

Figure 2. (a) Relation between the relaxation rate constant, $k_1(i)$, and photon energy, E_p, for different Rb/THF solutions: (1) freshly-prepared; (2) 1-day old; (3) 3-days old. Best-fit analysis was carried out with eq 2 as described in the text. (b) Energetics of a typical Rb/THF solution, focusing on Rb^- and THF. The energy of Rb^- was estimated via eq 8, E_c is the mobility edge (also known as V_0, see ref. 11), E_{th} is the experimental value of the threshold energy taken from the best-fit analysis (eq 2 and Figure 2a), and E_s is the energy of the hydrated electron (ref 21). Notice the parabolic shape of the conduction band (dashed line) which corresponds to the experimental parabolic dependence shown in Figure 2a.

effects and also to treat pure exponential decays, namely

$$\ln\frac{I}{I_0}(i) = -k_1(i)\tau_d \qquad (1)$$

where $k_1(i) = 1/T_1(i)$ is the spin relaxation rate constant which is plotted for different samples, i, and photon energies, E_p (in Figure 2a).

The conspicuous decreases in $k_1(i)$ upon increase of the excitation wavelength can be interpreted semiqualitatively by the following analytical description

$$k_1(i) = 1/T_1(i) = k_{10}(i) + A(E_p - E_{th}')^{1/2} \qquad (2)$$

where $k_{10}(i)$ is a parameter independent of E_p but depends on sample conditions. For example, for a freshly prepared sample $k_{10} = 0$, while for samples that were stored for a longer period (a few days) $k_{10} > 0$.[7] The apparent threshold energy, E_{th}', and the constant parameter A were obtained by the curve fitting, with values of 1.59 ± 0.10 eV and 0.19 ± 0.01 μs^{-1} $eV^{-1/2}$, respectively. The shifts within the curves (Figure 2a) are due to different k_{10} values. It is noteworthy that the k_1 value obtained for a freshly prepared sample is in agreement with previous results taken at $\lambda = 532$ nm only.[5] The justification for using eq 2 in the analysis of the results will be given in the next sections.

Energetic of Rb/THF Solutions. Figure 2b represents the energy scheme of Rb/THF solution and the processes that are associated with photoexcitation. In reference to this scheme, several points are discussed.

1. For noncrystalline media as liquids, the distribution of energy states does not differ considerably from the corresponding distribution in a crystal.[8] With this concept, the valence and conduction bands of THF are presented in Figure 2b. In this scheme $N(E)\,dE$ is the number of states per unit volume available for an electron possessing energy between E and $E + dE$. Each energy band in amorphous material can be divided into two regions: (i) where the mean-free path, L, of the electron (characterized by its wavenumber, k) is large, i.e., $kL \gg 1$; (ii) where the interaction with phonons and impurities gives rise to strong scattering, i.e., a short mean-free path, $kL \approx 1$. In the former case, deviation of the density of states from the free-electron approach much be small, and thus, the density of states is given by:[8]

$$N(E) = \frac{km_e}{2\pi^2h^2} = \frac{m_e^{3/2}}{2^{1/2}\pi^2h^3}E^{1/2} \qquad (3)$$

The latter case occurs near the edges of the valence and conduction bands,[8] where the energy states are localized.[9] Anderson's localized states in the tails of the conduction and valence bands of THF are schematically shown in Figure 2b. A critical sharp energy, E_c (the mobility edge), separates the region having high mobility (μ_e) of delocalized electrons from that of the relatively low mobility of localized electrons. For electrons injected above E_c, metallic behavior is expected. In fact, a high mobility of electrons in electric fields has been observed in a number of liquids.[10] On the other hand, conductivity of localized electrons exhibits an activation energy, and their drift motion proceeds usually via thermally activated hopping.[11] As a rule, the E_c-value does not exceed a few tenths of an electronvolt above the conduction band edge.[8] The distance of E_c from the vacuum level (taken as zero energy) is also a few tenths of an electronvolt. Thus, for simplicity we take $E_c = -0.6$ eV, which is in line with E_c-values in other solutions.[12,13]

2. Dissolution of Rb in THF is accompanied by the reactions

$$2Rb^{\bullet}_{solid} \rightarrow Rb_s^+ + Rb_s^- \underset{k_d}{\overset{k_a}{\rightleftharpoons}} (Rb_s^+, Rb_s^-) \qquad (4)$$

where the subscript s stands for the solvated species. Since in nonirradiated solutions the solvated electron is not observed,[5] ion pairs which involved solvated electrons will not be considered. Unlike Rb_s^+, electrons can be detached from the stable species Rb_s^- by visible light, and this case will be considered.

If one does not account for ion-pair formation, the energy of Rb_s^-, relative to the vacuum, is given by[11]

$$E'_{Rb_s^-} = -EA + P_- \quad (5)$$

where EA is the electron affinity of RB$^\bullet$ (EA = 0.486 eV[14]) and P_- is the polarization energy of Rb^-, which can be estimated by Born's formula[15,16]

$$P_- = -\frac{e_0^2}{2R}\left[1 - \frac{1}{\epsilon_s}\right] \quad (6)$$

where e_0 is the electron charge, R is the ionic radius including the first solvation shell,[17] and ϵ_s is the static dielectric constant, which is 11.5 for THF at 180 K.[18] Thus, for $R = 6$ Å,[19] $P_- = -1.2$ eV. Because of the ion−pair formation (Rb_s^+, Rb_s^-), the Coulombic term should also be considered[16]

$$C = e_0^2\left[\frac{R}{2d^2} + \frac{1}{d\epsilon_s}\left(1 - \frac{R}{d}\right)\right] \quad (7)$$

where d is the distance between ions in the pair and the constant 2 is related to the refractive index. A reasonable ratio of $d/R = 1.5$ results in $C \approx 0.6$ eV. The energy level of Rb^- (relative to the vacuum) is calculated to be

$$E_{Rb_s^-} = E'_{Rb_s^-} - C \approx -2.3 \text{ eV} \quad (8)$$

and is shown in Figure 2b with a Gaussian distribution, reflecting the temporal fluctuation of a single energy level of Rb^-.[20]

3. Electrons in the conduction band are more energetic than solvated electrons, e_s^-. Thus in time course, the former should transform into solvated species.[21] Nevertheless, and in line with previous results, no solvated electrons could be detected at low Rb^- concentration ($Rb^- \leq 10^{-4}$ M), even after a few minutes of laser irradiation (tens of thousands of laser shots).[5,22] Detection of solvated electrons by EPR becomes possible at higher Rb^- concentrations, especially upon addition of chelates.[3−5] So far, there is no adequate mechanism that accounts for the absence of detectable solvated electrons at low Rb^- concentration. It is conceivable that the life time e_s^- is too short, probably due to a quenching mechanism that may involve rubidium cations. Chelates, on the other hand, prevent such a process due to their screening effects.

Photodetachment. In the gas phase, photodetachment (pd) from Rb^-, at ~600 nm, proceeds with approximately equal probability either to the excited Rb$^\bullet$($^2P_{1/2,3/2}$) states, yielding slow electrons, or to the Rb$^\bullet$($^2S_{1/2}$) ground state, ejecting very fast electrons.[22] In solution, due to solute−solvent interactions, the energy level of Rb_s^-($^1S_0$) is blue-shifted and 500−700 nm excitation yields the ground state, Rb$^\bullet$($^2S_{1/2}$), namely

$$(Rb_s^+, Rb_s^-(^1S_0)) + h\nu \xrightarrow{k_{pd}} Rb_s^+ + Rb^\bullet(^2S_{1/2}) + e_p^- \quad (9)$$

The concentration of the products is given by

$$[e_p^-] = [Rb^\bullet] = k_{pd}[(Rb_s^+, Rb_s^-)]\tau_{1p} \quad (10)$$

where k_{pd} is the rate constant of photodetachment and $\tau_{1p} = 12$ ns is the laser-pulse duration. k_{pd} can be expressed as $k_{pd} = \sigma_{pd}J$, where σ_{pd} is the cross section of the photoprocess and J is the photon flux through a unit area during the laser pulse ($J = W_1/(E_pA_1)$ where W_1 is the laser pulse energy and A_1 is the cross-sectional area of the laser beam) and $[e_p^-] \approx (3-10) \times 10^{12}$ cm^{-3} is the concentration of ejected photoelectrons, detected by EPR.[5]

Electron ejection, via photodetachment, from sodium anion dissolved in hexamethylphosphoric triamide[23] and anthracene anion in THF[24] consists of direct bound−continuum transitions and bound−bound transitions with autoionization into continuum. Inspection of Figure 2b points out that bound−continuum transitions (direct or via autoionization) can also occur in Rb/THF.

The cross section for photodetachment into the conduction band continuum is given by[25,26]

$$\sigma_{pd} \approx E_p|\langle\Psi_d|\vec{P}|\Psi_c\rangle|^2 N(E_p - E_{th}) \quad (11)$$

where E_{th} is the energy distance between Rb^- and the threshold of the parabolic conduction band of THF. In the free electron model approximation, $(E_p - E_{th})$ is the kinetic energy of quasi-free electrons, $N(E_p - E_{th})$ is the density of states in the conduction band, Ψ_d and Ψ_c are the electron wave functions in initial discrete and final continuum states, and $\vec{P}$ is the electric dipole operator of Rb^-. Combining eqs 3, 10, and 11 results in the expression for the photodetachment yield

$$[e_p^-] = [Rb^\bullet] = aJE_p(E_p - E_{th})^{1/2}[(Rb_s^+, Rb_s^-)]\tau_{1p} = b(E_p - E_{th})^{1/2} \quad (12)$$

where a and b are constants to be matched with our experimental conditions and E_{th} can be directly related to E_{th}' (eq 2). For all samples, best-fit lines exhibit the same parabolic dependence upon E_p, which corresponds to the conduction band profile (indicated by the dashed curve) in Figure 2b.

Spin Relaxation Mechanism. The parallel relaxation channels in eq 2 can be rewritten as

$$k_1(i) = k_{10}(i) + k_1(E_p) = 1/T_1(i) = 1/T_{10}(i) + 1/T_1(E_p) \quad (13)$$

The first channel[7] indicates a slow reaction (probably with impurities). However, the wavelength-dependent relaxation term warrants further discussion.

In the conduction band of metals, the dominant relaxation mechanisms are due to spin exchange via electron−electron collisions and electron scattering on paramagnetic centers.[27] Because of the high mobility of the conduction electrons, electron dipole−dipole and electron−nuclear hyperfine interactions are effectively averaged to zero.

In Rb/THF, both paramagnetic species, i.e., the electron and rubidium atoms, are generated via photodetachment (eq 9). Taking into account electron−electron and electron−rubidium scattering, a rate constant of the longitudinal spin relaxation can be expressed as

$$\frac{1}{T_1} = k_1(E_p) = 4\pi D_e\{p_eR_e[e_p^-] + p_rR_r[Rb^\bullet]\} = 4\pi D_e[e_p^-]\{p_eR_e + p_rR_r\} \quad (14)$$

where D_e is the diffusion coefficient of the photoelectron, R_e and R_r are the collision distances for electron−electron and electron−atom pairs, and p_e and p_r are the probabilities of spin relaxation per collision. Since quasi-free electrons are devoid of a solvent shell, $R_r \gg R_e$ must be fulfilled, and eqs 12 and 14 result in

$$k_1(E_p) \approx 4\pi p_rR_rD_e[e_p^-] = 4\pi p_rR_rD_eb(E_p - E_{th})^{1/2} = A(E_p - E_{th})^{1/2} \quad (15)$$

which is the theoretical derivation that coincides with the relation given by eq 2 (cf. Figure 2a).

On the basis of the experimental values of k_1 and $[e_p^-]$ and assuming that $R_r \approx 10^{-7}-10^{-6}$ cm, we can estimate the product

$p_r D_e$ in eq 15 to be $10^{-3}-10^{-2}$ cm^2/s. Since $p_r \leq 1$, we obtain that $D_e \geq 10^{-3}$ cm^2/s. The mobility of the electrons can be estimated through Einstein's relation[28]

$$\mu_e = \frac{e_0 D_e}{k_B T} \tag{16}$$

where μ_e is the electron mobility in the electric field. This approximation results in the inequality $\mu_e \geq 0.1$ cm^2/Vs.[29] This value is higher than for solvated electrons in THF (3×10^{-3} cm^2/Vs)[30] but lower than for electrons in a different ether, hexamethyldisiloxane (22 cm^2/Vs).[10] Measurements carried out at high temperature point out that a conduction band exists in ethers.[30] Probably, the mobility of photoelectrons in THF and other ethers is associated with the two-state model, where electron jumps between delocalized and localized states with relatively large fraction of the time in the delocalized conduction band.[10,31]

Conclusion

To realize spin transfer (transfer of spin polarization) through the liquid/solid interface, two essential conditions should be fulfilled. The first condition requires that the probability of spin flip onto the surface be low. Apparently, this requirement is being fulfilled in our system. For metals, such a probability which allows spin transfer in the metal−metal interface, as recently demonstrated by Johnson,[1c] is of $10^{-6}-10^{-5}$.[27] The second condition, namely sufficiently high mobility of spin carriers in liquid, is also feasible according to the results of the present study utilizing photoelectrons as carriers.

Acknowledgment. We are grateful to Dr. Holroyd who provided us with a preprint of ref 10. This work was supported by grants from The Israel Science Foundation and The Israel Ministry of Energy and Infrastructure. The support of the Giladi Fund (V.R.) is highly appreciated. The Farkas Research Center is supported by the Minerva Gesellschaft für die Forschung, GmbH, München, FRG. This work is in partial fulfillment of the requirements for a Ph.D. degree (Y.H.) at the Hebrew University of Jerusalem.

References and Notes

(1) (a) Aronov, A. G. *JETP Lett*. **1976**, *24*, 32. (b) Silsbee, R. H. *Bull. Magn. Reson*. **1980**, *2*, 284. (c) Johnson, M. *Science* **1993**, *260*, 320.

(2) Unpublished results from our laboratory.

(3) (a) Friedenberg, A.; Levanon, H. *Chem. Phys. Lett*. **1976**, *41*, 84. (b) Friedenberg, A.; Levanon, H. *J. Phys. Chem*. **1977**, *81*, 766. (c) Eliav, U.; Levanon, H. *Chem. Phys. Lett*. **1978**, *55*, 369. (d) Eliav, U.; Levanon, H. *Chem. Phys. Lett*. **1980**, *72*, 213. (e) Eliav, U.; Levanon, H. *J. Phys. Chem*. **1980**, *84*, 842. (f) Eliav, U.; Levanon, H.; Carton, P. M.; Fessenden, R. W. *Chem. Phys. Lett*. **1981**, *82*, 365.

(4) Eliav, U.; Freed, J. H. *J. Phys. Chem*. **1984**, *88*, 1277. The wavelength dependence of risetime of electron spin polarization has been observed in this work.

(5) Rozenshtein, V.; Zilber, G.; Levanon, H. *J. Phys. Chem*. **1994**, *98*, 4236.

(6) Dye, J. L.; Andrews, C. W.; Mathews, S. E. *J. Phys. Chem*. **1975**, *79*, 3065.

(7) In our experiments k_{10} (1) = 0.00 ± 0.01 μs^{-1}; k_{10} (2) = 0.05 ± 0.01 μs^{-1}; k_{10} (3) = 0.11 ± 0.01 μs^{-1}.

(8) (a) Mott, N. F.; Davis, E. A. *Electronic processes in non-crystalline materials*; Clarendon Press: Oxford, 1971. (b) Mott, N. F. *Metal-insulator transitions*, 2nd ed.; Taylor and Francis: London, 1990. (c) Mott, N. F. *Conduction in non-crystalline materials*, 2nd ed.; Clarendon Press: London, 1993.

(9) Anderson, P. W. *Phys. Rev*. **1958**, *109*, 1492.

(10) E.g., μ_e = 100 cm^2/Vs in tetramethylsilane (Bakale, G.; Beck, G. *J. Chem. Phys*. **1986**, *84*, 5344), μ_e = 63 cm^2/Vs in bis(trimethylsilyl)-methane, and μ_e = 22 cm^2/Vs in hexamethyldisiloxane (R. A. Holroyd, K. Itoh, M. Nishikawa, *Nucl. Instrum. Methods Phys. Res. A*, in press.

(11) (a) Schmidt, W. F. *Can. J. Chem*. **1977**, *55*, 2197. (b) Schmidt, W. F. In *Excess electrons in dielectric media*; Ferradini, C., Jay-Gerin, J.-P., Eds.; CRC Press: Boca Raton, FL, 1992; pp 127−159.

(12) For example, in TMS E_c = −0.56 eV, in neopentane E_c = −0.45 eV (Holroyd, R. A.; Gangwer, T. E. *Radiat. Phys. Chem*. **1980**, *15*, 283), and in isooctane E_c = −0.19 eV (Balakin, A. A.; Boriev, I. A.; Jakovlev, B. S. *Can. J. Chem*. **1977**, *55*, 1985).

(13) In the theory of ion mobility in liquids, E_c is often denoted as V_0 and is called the energy of the delocalized excess electron state.

(14) Radzig, A. A.; Smirmov, B. M. *Reference data on atoms, molecules and ions*; Springer-Verlag: Berlin, 1985.

(15) Born, M. *Z. Phys*. **1920**, *1*, 45.

(16) Suppan, P. *Chimia* **1988**, *42*, 320.

(17) Purcell, K. F.; Blaive, B. In *Photoinduced electron transfer*; Fox, M. A., Channon, M., Eds.; Elsevier: Amsterdam, 1988; pp 123−129.

(18) Marcus, Y. *Ion solvation*; Wiley: Chichester, 1985.

(19) Rozenshtein, V.; Zilber, G.; Rabinovitz, M.; Levanon, H. *J. Am. Chem. Soc*. **1993**, *115*, 5193.

(20) Gerischer, M. *Z. Phys. Chem., Neue Folge* **1960**, *26*, 325.

(21) The energy localization of e_s^- in THF is not known, whereas the hydrated electron is located at −1.7 eV: Bockris, J. O. M.; Khan, S. U. M. *Quantum Electrochemistry*; Plenum Press: New York, 1979; p 413.

(22) Frey, P.; Lawen, M.; Breyer, F.; Klar, H.; Hotop, H. *Z. Phys. A: At. Nucl*. **1982**, *304*, 155.

(23) Aulich, H.; Nemec, L.; Delahay, P. *J. Chem. Phys*. **1974**, *61*, 4235.

(24) Aulich, H.; Baron, B.; Delahay, P. *J. Chem. Phys*. **1973**, *58*, 603.

(25) Branscomb, L. M. In *Atomic and molecular processes*; Bates, D. R., Ed.; Academic Press: New York, 1962; pp 100−140.

(26) Rozenshtein, V. B., Gershenzon, YuM., Nalbandian, A. B., Eds. *Magnetic resonance in gases*; Academy of Sciences: Erevan, 1987.

(27) Salikhov, K. M.; Semenov, A. G.; Tzvetkov, YuD. *Electron spin echo and its application*; Nauka: Novosibirsk, 1976.

(28) Morrison, S. R. *Electrochemistry of semiconductor and oxidized metal electrodes*; Plenum Press: New York, 1980.

(29) Recently, we have carried out direct measurements of the photoelectron mobility in THF finding that $\mu_e \approx 0.1-1$ cm^2/Vs. To correlate this results with our findings reported here, $p_r \approx 1$ and $D_e \approx 10^{-3}-10^{-2}$ cm^2/s.

(30) Dodelet, J. P.; Freeman, G. R. *Can. J. Chem*. **1975**, *53*, 1263.

(31) Freeman, G. R. In *The liquid state and its electrical properties*; Kunhardt, E. E., Christophorou, L. G., Luessen, L. H., Eds.; Plenum Publishing: New York, 1988; pp 251−272.